

Electrical, magneto-, and optical conductivity of quasicrystals in the Al-Re-Pd system

A. D. Bianchi, F. Bommeli, M. A. Chernikov, U. Gubler, L. Degiorgi, and H. R. Ott

Laboratorium für Festkörperphysik, Eidgenössische Technische Hochschule Hönggerberg, CH-8093 Zürich, Switzerland

(Received 11 July 1996)

Measurements of the electrical conductivity $\sigma(T)$ and magnetoconductivity $\Delta\sigma(H)$ of icosahedral $\text{Al}_{70}\text{Re}_{10}\text{Pd}_{20}$ and $\text{Al}_{70}\text{Re}_{8.6}\text{Pd}_{21.4}$ quasicrystals at low temperatures and in high magnetic fields H are reported. Below 0.2 K, σ of $\text{Al}_{70}\text{Re}_{10}\text{Pd}_{20}$ varies as $\sigma(T) = \sigma_0 + aT^{1/2}$ with $\sigma_0 = 30 \Omega^{-1} \text{cm}^{-1}$ and $a < 0$. The conductivity decreases with increasing magnetic field. For $\text{Al}_{70}\text{Re}_{8.6}\text{Pd}_{21.4}$ $\sigma(T)$ decreases with decreasing T and saturates at the level $\sigma_0 = 1.7 \Omega^{-1} \text{cm}^{-1}$ below 0.1 K. In magnetic fields up to 40 kOe, $\Delta\sigma(H)$ is negative below 1 K and $\sigma(T, H)$ remains temperature-independent at the lowest temperatures. The optical conductivity $\sigma(\omega)$ is obtained from reflectivity data in the frequency range between 15 and 10^5cm^{-1} . The main contributions to $\sigma(\omega)$ are a broad absorption signal centered at about 0.1 eV and a sizable peak with its maximum at 2.6 eV. [S0163-1829(97)03310-9]

I. INTRODUCTION

Among thermodynamically stable quasicrystals, icosahedral Al-Re-Pd is a quasiperiodically structured material which often shows very low values of the electrical conductivity at low temperatures, comparable to those observed in heavily doped semiconductors.¹ It seems possible to synthesize icosahedral Al-Re-Pd samples with different chemical composition and annealing procedures while maintaining about the same structural properties. The low-temperature values of the electrical conductivity of these alloys vary over three orders in magnitude.² Therefore icosahedral quasicrystals in the Al-Re-Pd system may be considered as model substances for investigating electronic transport properties both at zero and nonzero frequency of quasiperiodically ordered solids with varying concentration of itinerant charge carriers.

The available information on electrical-transport properties of these materials includes data of the electrical d.c. conductivity $\sigma(T)$ and the magnetoconductivity $\Delta\sigma(H)$,²⁻⁵ as well as $\sigma(\omega)$ data obtained from reflectivity measurements.⁶ Below we describe our results of measurements of the dc electrical conductivity $\sigma(T)$ and magnetoconductivity $\Delta\sigma(H)$ of two samples of quasicrystalline Al-Re-Pd with different composition in overlapping temperature ranges between 0.04 and 295 K. This set of data extends the temperature range of previous measurements to considerably lower temperatures. We also present the results of reflectivity measurements and the resulting $\sigma(\omega)$ behavior in the frequency range between 15 and 10^5cm^{-1} at different temperatures between 6 and 300 K. In this work, besides covering a more extended frequency range than in a previous investigation,⁶ also the effect of the variation of the chemical composition on $\sigma(\omega)$ for these Al-Re-Pd quasicrystals is investigated.

II. SAMPLES AND EXPERIMENT

We have synthesized samples with nominal compositions $\text{Al}_{70}\text{Re}_{10}\text{Pd}_{20}$ and $\text{Al}_{70}\text{Re}_{8.6}\text{Pd}_{21.4}$ from 99.999% pure alumi-

num, 99.9975% pure palladium, and 99.94% pure rhenium by arc melting suitable amounts of the constituent elements to a single piece in an argon atmosphere and remelting it several times. The resulting ingots were annealed in vacuum for 2 days and subsequently rapidly cooled to room temperature. Powder x-ray diffraction and surface analysis with back-scattered electron images confirmed the absence of inclusion of other phases. Selected-area electron-diffraction patterns revealed a high degree of structural order. The specimens in the form of prisms with approximate dimensions $0.8 \times 1.4 \times 6 \text{mm}$ were cut from the ingots using spark-erosion.

The electrical conductivity $\sigma(T)$ and the magnetoconductivity $\Delta\sigma(H)$ of icosahedral $\text{Al}_{70}\text{Re}_{10}\text{Pd}_{20}$ and $\text{Al}_{70}\text{Re}_{8.6}\text{Pd}_{21.4}$ were measured using a standard four probe ac technique at low frequency. The measurements of the electrical conductivity $\sigma(T)$ covered the temperature range between 0.04 and 295 K. The magnetoconductivity $\Delta\sigma(H)$ was measured at temperatures between 0.04 and 1.2 K and in magnetic fields up to 56 kOe.

The reflectivity $R(\omega)$ as a function of temperature has been measured for the same samples within a broad frequency range between 15 and 10^5cm^{-1} , using four spectrometers with overlapping frequency ranges.⁷ In the far infrared (FIR) we made use of a Bruker IF113v Fourier interferometer with a Hg arc-light source and a He-cooled Ge-bolometer detector, while from the FIR up to the mid-IR range a fast scanning Bruker interferometer IFS48PC was used. In the visible spectral range a homemade spectrometer based on a Zeiss monochromator was employed and in the ultraviolet we used a McPherson spectrometer. From the mid-IR down to the FIR we have used the reflectivity of tungsten as reference. The specimens had two large rectangular shiny surfaces. Subsequently, the surfaces of both samples were polished and measured again, without a noticeable change of $R(\omega)$, neither qualitatively nor quantitatively, besides an irrelevant increase of the overall reflectivity of a few percent.

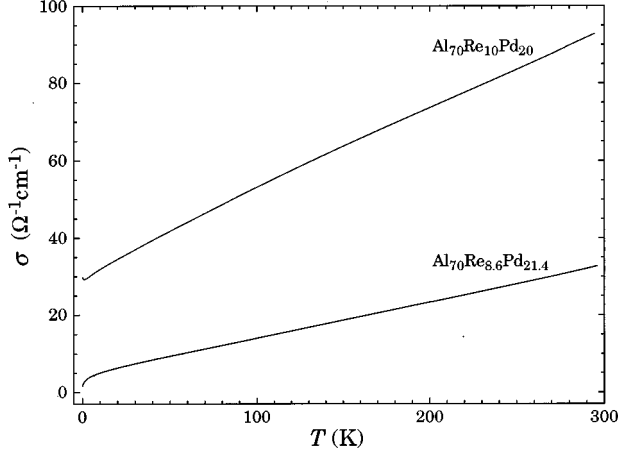


FIG. 1. Electrical conductivity $\sigma(T)$ of $\text{Al}_{70}\text{Re}_{10}\text{Pd}_{20}$ and $\text{Al}_{70}\text{Re}_{8.6}\text{Pd}_{21.4}$ between 0.04 and 295 K.

III. RESULTS AND ANALYSIS

A. dc conductivity and magnetoconductivity

The electrical conductivity $\sigma(T)$ of both $\text{Al}_{70}\text{Re}_{10}\text{Pd}_{20}$ and $\text{Al}_{70}\text{Re}_{8.6}\text{Pd}_{21.4}$ measured in zero magnetic field H below room temperature is shown in Fig. 1. In both cases, the electrical conductivity σ first decreases with a constant slope $d\sigma/dT$ with decreasing temperature. The range of temperature for which $d\sigma/dT$ is approximately constant extends to 170 K for $\text{Al}_{70}\text{Re}_{10}\text{Pd}_{20}$ and 40 K for $\text{Al}_{70}\text{Re}_{8.6}\text{Pd}_{21.4}$ and the respective values are 0.2 and $0.09 \text{ } \Omega^{-1} \text{ cm}^{-1} \text{ K}^{-1}$. The room temperature conductivities differ by a factor of 3 but the ratio of the limiting low-temperature values of σ is approximately 18. In both cases, it is not *a priori* obvious what causes the enhanced reduction of σ at low temperatures. Distinctly different features of $\sigma(T)$ of the two alloys are also observed at very low temperatures and we present and discuss the two cases separately.

In Fig. 2 we display a plot of σ vs $T^{1/2}$ in different external magnetic fields for $\text{Al}_{70}\text{Re}_{10}\text{Pd}_{20}$. For $H=0$ we recog-

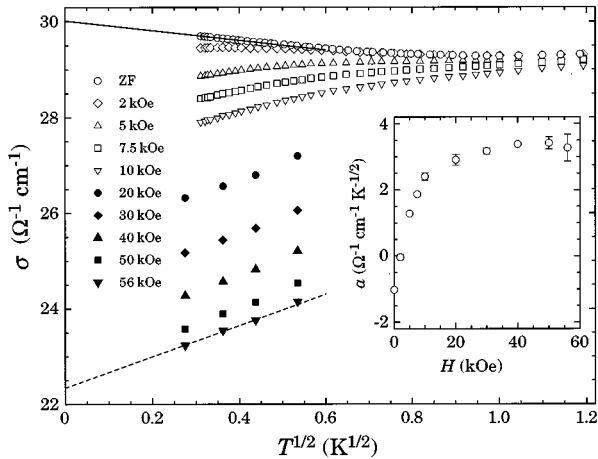


FIG. 2. Electrical conductivity σ of icosahedral $\text{Al}_{70}\text{Re}_{10}\text{Pd}_{20}$ below 1 K in varying magnetic fields H plotted as a function of $T^{1/2}$. The lines represent the fits of Eq. 1 to the $\sigma(T)$ data between 0.1 and 0.2 K (see text). Inset: $d\sigma/d(T^{1/2})$ vs H .

nize a minimum of $\sigma(T)$ at approximately 1 K. Below 0.2 K, the electrical conductivity $\sigma(T, H=0)$ varies as

$$\sigma(T) = \sigma_0 + aT^{1/2}, \quad (1)$$

and an extrapolation of our $\sigma(T)$ data to $T=0$, shown as the solid line in Fig. 2, yields the residual conductivity $\sigma_0 = 30 \text{ } \Omega^{-1} \text{ cm}^{-1}$ and the slope $a = -1.02 \text{ } \Omega^{-1} \text{ cm}^{-1} \text{ K}^{-1/2}$. Upon application of an external magnetic field the negative slope of the $T^{1/2}$ variation at the lowest temperatures decreases in magnitude and changes sign at approximately 2 kOe (see inset). Below 0.2 K and in magnetic fields $H > 5 \text{ kOe}$, the electrical conductivity $\sigma(T)$ varies still as $T^{1/2}$, but with a positive slope a . In this regime the observed magnetoconductivity $\Delta\sigma(H) = \sigma(H) - \sigma(0)$ is negative. In the inset of Fig. 2 we plot the slope a resulting from the fits of Eq. 1 to our $\sigma(T)$ data taken in various magnetic fields H in the temperature range between 0.075 and 0.2 K, as a function of H . As mentioned above, a increases gradually with increasing H and changes sign at about 2 kOe. For magnetic fields exceeding 20 kOe, $a(H)$ tends to saturate, reaching a value of $3.27 \text{ } \Omega^{-1} \text{ cm}^{-1} \text{ K}^{-1/2}$ at $H = 56 \text{ kOe}$.

In the following we analyze these $\sigma(T, H)$ variations with respect to T and H in terms of quantum-interference effects considering Coulomb interactions among itinerant electrons.^{8,9} It should be noted that quantum-interference contributions to the electrical conductivity should also include weak-localization terms.¹⁰ The plots in Fig. 2 indicate that below 0.2 K, $\sigma(T)$ is adequately described by Eq. (1), suggesting that the temperature dependence of σ is predominantly determined by a Coulomb-type interaction correction to the classical Boltzmann conductivity. Similar behavior of the electrical conductivity at low temperatures has previously been observed for various icosahedral quasicrystals.⁴

In the case of a single isotropic band the Coulomb interaction corrections $\delta\sigma_I^{\text{ZF}}$ and $\delta\sigma_I^{\text{HF}}$ to the classical conductivity in zero magnetic field $H=0$ and in the limit of high magnetic field $g\mu_B H \gg k_B T$, respectively, are⁸

$$\delta\sigma_I^{\text{ZF}}(T) = \frac{e^2}{4\pi^2\hbar} \frac{1.3}{\sqrt{2}} \left(\frac{4}{3} - \frac{3}{2}\tilde{F}_\sigma \right) \left(\frac{k_B T}{\hbar D} \right)^{1/2}, \quad (2)$$

$$\delta\sigma_I^{\text{HF}}(T) = \frac{e^2}{4\pi^2\hbar} \frac{1.3}{\sqrt{2}} \left(\frac{4}{3} - \frac{1}{2}\tilde{F}_\sigma \right) \left(\frac{k_B T}{\hbar D} \right)^{1/2}. \quad (3)$$

Here \tilde{F}_σ is the Coulomb screening parameter and D is the electron diffusion constant.⁹ Solving the system of Eqs. (2) and (3) for \tilde{F}_σ and D using the $d\sigma/d(T^{1/2})$ values obtained in the way described above yields $\tilde{F}_\sigma = 1.1$ and $D = 0.26 \text{ cm}^2 \text{ s}^{-1}$. We note that \tilde{F}_σ values exceeding 0.92 are not really compatible with a first-order perturbation theory considering a single isotropic band,⁸ but values of \tilde{F}_σ exceeding 0.92 have previously been reported for heavily doped semiconductors^{11,12} and for icosahedral quasicrystals.⁴ In both cases a single isotropic band is not necessarily a good approximation. We also note an unusually high value of D for a material with $\sigma_0 = 30 \text{ } \Omega^{-1} \text{ cm}^{-1}$, suggesting a very low density of electronic states at E_F .

In principle an independent evaluation of the electron diffusion constant D may be made using the Einstein relation for the electrical conductivity $\sigma_B = e^2 N(E_F) D$, where σ_B is the classical Boltzmann conductivity and $N(E_F)$ is the density of electronic states at the Fermi level. The latter quantity may be obtained from the coefficient γ_{el} of the electronic specific heat $\gamma_{el} T$. We note, however, that the large residual conductivity ratio of $\text{Al}_{70}\text{Re}_{10}\text{Pd}_{20}$ may lead to a considerable difference between the residual conductivity σ_0 and the Boltzmann conductivity σ_B at zero temperature and, consequently, to an uncertainty in the estimate of the electron diffusion constant D .

For Al-Re-Pd quasicrystals a reliable evaluation of $N(E_F)$ from the electronic contribution $\gamma_{el} T$ to the specific heat $C_p(T)$ is obscured by the presence of tunneling states as indicated by the results of our thermal-conductivity measurements on the same materials.¹³ Analyzing the tunneling state model^{14,15} and assuming a frequency-independent density of tunneling states, thermal excitations of these states are expected to contribute a term $\gamma_{TS} T$ to the total specific heat $C_p(T)$. Tunneling states are commonly present in metallic glasses and their contribution C_{TS} to the specific heat $C_p(T)$ is typically of the order $50 T \mu\text{J g-atom}^{-1} \text{K}^{-1}$.¹⁶ This $\gamma_{TS} T$ value corresponds to approximately 1/3 of the linear contribution $\gamma T = 139 T \mu\text{J g-atom}^{-1} \text{K}^{-1}$ to $C_p(T)$ of this particular $\text{Al}_{70}\text{Re}_{10}\text{Pd}_{20}$ alloy.¹⁷ Assuming that $\sigma_B = \sigma_0$ and that $\gamma_{el} = \frac{2}{3} \gamma$, we obtain $D = 0.071 \text{ cm}^2 \text{ s}^{-1}$, i.e., a factor of four smaller value than the D value obtained in the way described above. Inserting this value in Eq. (2) results in $\tilde{F}_\sigma = 0.98$.

The Coulomb interaction corrections to the electrical conductivity, as given by Eqs. (2) and (3) have been obtained for the case of a single isotropic band. Recently Burkov and co-workers^{18–20} have proposed a model for the band structure of quasicrystals based on the explicit assumption of nearly free electrons close to a Fermi surface. They have argued that for a Hume-Rothery-type electronic stabilization mechanism the interaction of the Bragg planes with the Fermi surface results in an almost complete collapse of the latter. Within this scenario, the only pieces of the Fermi surface to survive are pockets of electrons and holes determined by the ratio of the Fermi wave vector k_F and the reciprocal lattice vectors associated with the strongest structure factors. The generalization of Eq. (2) to a many-pocketed Fermi surface has previously been discussed in detail for heavily doped semiconductors.^{11,12} In the case of a Fermi surface that consists of n valleys identically oriented in reciprocal space and negligible intervalley scattering, the factor 3/2 in front of \tilde{F}_σ in Eq. (2), which gives the zero-field correction to $\sigma(T)$ resulting from the interaction of a particle and a hole with total spin $j = 1$, needs to be replaced by $(2n - \frac{1}{2})$.⁸ For the case of strong intervalley scattering the quantum correction to the electrical conductivity $\sigma(T)$ is expected to have the same form as for a single isotropic band.⁸

The anisotropy of a nonspherical Fermi surface is also expected to modify the quantum corrections, as it leads to anisotropic diffusion of electrons and holes. The electron-electron interaction effects result from particle diffusion, as a consequence they will possess the same anisotropy as the diffusion coefficient.⁸ The spherical symmetry of the prob-

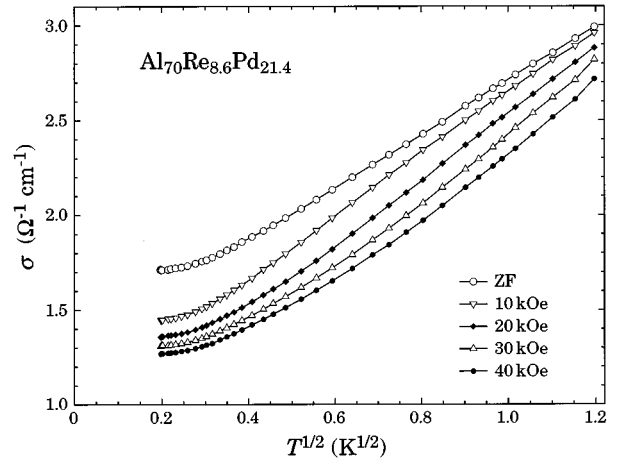


FIG. 3. σ vs $T^{1/2}$ for icosahedral $\text{Al}_{70}\text{Re}_{8.6}\text{Pd}_{21.4}$ below 1 K in varying magnetic fields H . The lines are to guide the eye.

lem can be restored by deforming the frame associated with the main axes of the diffusion coefficient tensor ellipsoid. The diffusion coefficient D in Eqs. (2) and (3) has to be replaced by $D_a = (D_\perp^2 D_\parallel)^{1/3}$. The correction to the electrical conductivity $\Delta\sigma$ should then be multiplied by the factor D_{ik}/D_a ,⁸ where D_{ik} is the classical diffusion tensor. Experiments probing the magnetoconductivity dependence on the orientation between the symmetry axes of a quasicrystal and the applied magnetic field using single-grained samples, as has been done for arsenic doped germanium,²¹ would be helpful for estimating the importance of these anisotropies.

We now present and discuss the temperature and the magnetic field dependencies of the electrical conductivity σ of $\text{Al}_{70}\text{Re}_{8.6}\text{Pd}_{21.4}$ and compare them with the results for $\text{Al}_{70}\text{Re}_{10}\text{Pd}_{20}$ described above. The electrical conductivity $\sigma(T)$ of $\text{Al}_{70}\text{Re}_{8.6}\text{Pd}_{21.4}$, shown in Fig. 1, continues to decrease monotonically with decreasing temperature and below 0.1 K it saturates at the level of $\sigma_0 = 1.7 \text{ } \Omega^{-1} \text{ cm}^{-1}$. This type of $\sigma(T)$ behavior is distinctly different from that of $\text{Al}_{70}\text{Re}_{10}\text{Pd}_{20}$ (see above). In Fig. 3 the low-temperature electrical conductivity $\sigma(T)$ of $\text{Al}_{70}\text{Re}_{8.6}\text{Pd}_{21.4}$ is shown as a function of $T^{1/2}$ for $T < 1.5$ K and in applied magnetic fields up to 40 kOe. Between 0.04 and 1.5 K, the measured magnetoconductivity $\Delta\sigma = \sigma(H) - \sigma(0)$ is negative and fairly large. For $T = 0.04$ K and $H = 40$ kOe, e.g., $\Delta\sigma/\sigma = -0.3$, similar in magnitude as the analogous relative change of $\Delta\sigma/\sigma = -0.25$ for $\text{Al}_{70}\text{Re}_{10}\text{Pd}_{20}$. Below 0.1 K, $\sigma(T)$ approaches constant values for all applied magnetic fields up to 40 kOe, again in contrast to the $\sigma(T, H)$ behavior of $\text{Al}_{70}\text{Re}_{10}\text{Pd}_{20}$ described above. We note that the trend towards saturation of $\sigma(T)$ of $\text{Al}_{70}\text{Re}_{8.6}\text{Pd}_{21.4}$ at very low temperatures unambiguously implies a *metallic* ground state. On the other hand, the observed magnetic field and temperature-dependent features of σ of this material cannot be described using the above mentioned calculations⁹ considering quantum-interference effects including Coulomb interaction.

B. Reflectivity and optical conductivity

In principle, optical investigations, performed over a very broad spectral range, are a powerful experimental tool for identifying the spectrum of excitations. From this fairly com-

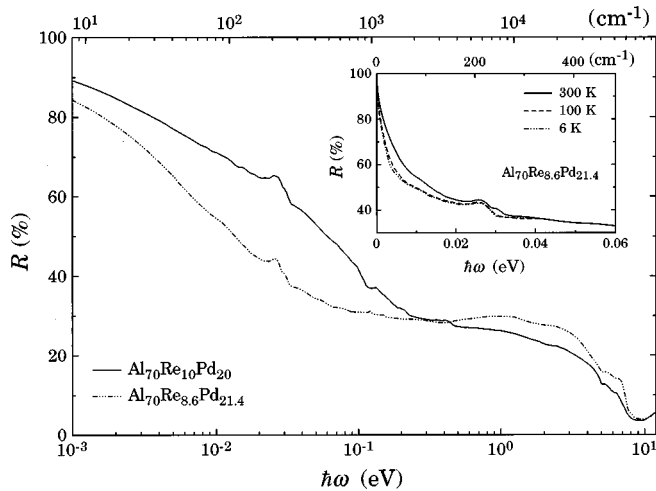


FIG. 4. Room-temperature reflectivity $R(\omega)$ for $\text{Al}_{70}\text{Re}_{10}\text{Pd}_{20}$ and $\text{Al}_{70}\text{Re}_{8.6}\text{Pd}_{21.4}$ for frequencies between 15 and 10^5 cm^{-1} . The inset displays $R(\omega)$ in the FIR spectral range for $\text{Al}_{70}\text{Re}_{8.6}\text{Pd}_{21.4}$ at various temperatures.

plete electrodynamic response several intrinsic parameters, such as, e.g., the plasma frequency and the scattering rate of the free charge carriers contribution, and the relevant excitations due to phonon modes or electronic transitions, may be extracted and evaluated.

Figure 4 displays the complete reflectivity spectra for both compounds at 300 K, while the inset shows the temperature dependence of $R(\omega)$ in the FIR spectral range for $\text{Al}_{70}\text{Re}_{8.6}\text{Pd}_{21.4}$. A similar weak temperature dependence was also found for $\text{Al}_{70}\text{Re}_{10}\text{Pd}_{20}$. At first sight, the spectra look metallic with a plasma-edge-type behavior at about 10 eV and an increasing reflectivity towards 100% for frequencies close to zero. A closer look reveals, however, a more complex behavior. There is definitely a broad shoulder in the visible spectral range and a distinct more narrow absorption in the FIR at about 0.02–0.03 eV. We also note that the less conducting sample reveals a less intense reflectivity below 0.2 eV, whereas the broad signal in the visible spectral range apparently acquires intensity for the less conducting alloy. Above 8 eV there is the clear onset of electronic interband transitions.

The complete set of optical properties expressed in terms of the complex optical conductivity is subsequently obtained via a Kramers-Kronig transformation (KK transformation) of the reflectivity spectrum. To this end, $R(\omega)$ was extrapolated to lower frequencies assuming a metallic behavior, thus using the Hagen-Rubens relation. Beyond the highest measurable frequency, we first used the extrapolation $R=1/\omega^2$, which simulates interband transitions, and at frequencies higher than $3.5 \times 10^5 \text{ cm}^{-1}$, we assumed $R=1/\omega^4$, simulating the behavior of free electrons.

Figure 5 shows the corresponding real part $\sigma_1(\omega)$ of the optical conductivity. From a very general point of view, the trend and shape of these results are very reminiscent of what has been found for $\text{Al}_{70}\text{Mn}_9\text{Pd}_{21}$.⁷ In fact, the FIR optical conductivity is very low and slightly increases with increasing frequency up to approximately 0.4 eV. An additional phononlike absorption at 0.02–0.03 eV is overlapping the low-frequency tail of the FIR $\sigma_1(\omega)$. At 0.4 eV, there is an

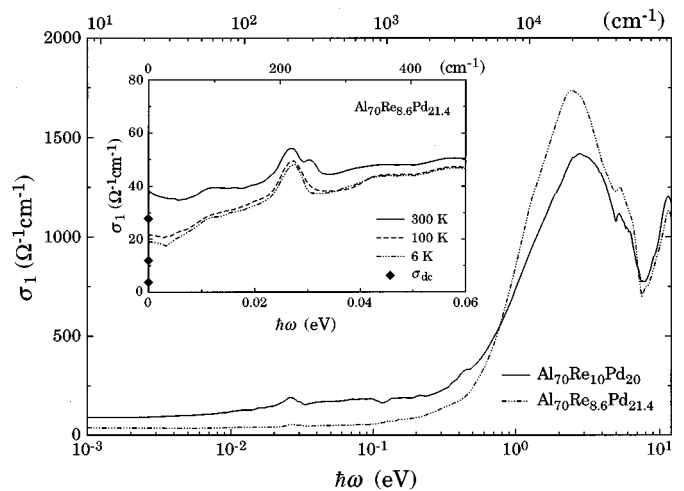


FIG. 5. Room temperature optical conductivity $\sigma_1(\omega)$ for $\text{Al}_{70}\text{Re}_{10}\text{Pd}_{20}$ and $\text{Al}_{70}\text{Re}_{8.6}\text{Pd}_{21.4}$ for frequencies between 15 and 10^5 cm^{-1} . The inset displays $\sigma_1(\omega)$ in the FIR spectral range for $\text{Al}_{70}\text{Re}_{8.6}\text{Pd}_{21.4}$ at various temperatures.

onset of a huge excitation centered at about 2.6–2.9 eV. The resonance frequency of this absorption is almost twice as high as that observed for the previously investigated $\text{Al}_{70}\text{Mn}_9\text{Pd}_{21}$ compound.⁷ We ascribe this absorption to excitations across a pseudogap in the density of states (DOS),⁷ which is believed to be a consequence of a Hume-Rothery-type electronic mechanism for stabilizing the quasicrystalline phase. The inset of Fig. 5 emphasizes the phonon mode and confirms the rather good agreement between the dc limit of $\sigma_1(\omega)$ and the dc transport result at 300 K. Nevertheless, at lower temperatures there is a systematic offset of $\sigma_1(\omega \rightarrow 0)$ with respect to σ_{dc} which is always lower. This feature was already recognized in a previous investigation.⁶ Our $R(\omega)$ and $\sigma_1(\omega)$ results roughly agree with those of Basov *et al.*⁶ on $\text{Al}_{70}\text{Re}_{10}\text{Pd}_{20}$ in the spectral range common to both studies, but both the intensity and the resonance frequency of the absorption at 2.6 eV revealed in our $\sigma_1(\omega)$ spectrum are sizeably different from those of Ref. 6. Our reflectivity data extend up to the UV and allow us to completely map the plasma-edge-like behavior of $R(\omega)$ and the high-frequency interband transitions. This is obviously of relevance for the KK transformations. Indeed, both the intensity and the resonance frequency of the broad signal in $\sigma_1(\omega)$ at about 2.6 eV depend very much on the high-frequency extrapolation. Therefore, the considerable difference in $\sigma_1(\omega)$ between our results and those of Ref. 6 can be ascribed to the fact that the authors of Ref. 6, for the purpose of the KK transformation, used our previous visible-UV data of the $\text{Al}_{70}\text{Mn}_9\text{Pd}_{21}$ material⁷ for extrapolating their data to higher frequencies.

The data displayed in the inset of Fig. 5 allow for an observation regarding the temperature variation of the lattice-mode feature of $\text{Al}_{70}\text{Re}_{8.6}\text{Pd}_{21.4}$. At room temperature this mode is split into two well separated peaks, merging into one single narrow peak at low temperatures. When subtracting the broad background manifested by the tail at low frequencies and extending up to the midinfrared spectral range it turns out that the spectral weight encountered in the double peak at 300 K is, within the experimental uncertainty, equal

to the spectral weight of the single absorption at low temperatures. Although not shown in detail, the same remarks are valid for $\text{Al}_{70}\text{Re}_{10}\text{Pd}_{20}$. This double-peak feature was also found in the excitation spectrum of $\text{Al}_{70}\text{Mn}_9\text{Pd}_{21}$ for which, however, it persisted down to low temperatures.⁷ Although we have no definite explanation for this peculiar temperature dependence of the lattice mode absorption of the Al-Re-Pd quasicrystals, we may anticipate that slight symmetry changes or temperature dependent coupling between the electronic and the lattice subsystems could lead to a redistribution of the spectral weight of the lattice modes.

For $\text{Al}_{70}\text{Mn}_9\text{Pd}_{21}$ the previously reported excitation spectrum of $\sigma_1(\omega)$ (Ref. 7) reveals a distinct double peak between 0.020 and 0.045 eV. This feature may be compared with the results of inelastic neutron-scattering experiments on Al-Mn-Pd quasicrystals. A time-of-flight experiment revealed a band of excitations centered at 0.016 eV and a broad maximum between 0.025 and 0.040 eV in the generalized density of vibrational states of icosahedral Al-Mn-Pd.²² An analogous investigation using a triple axis spectrometer has revealed a number of broad (0.004 eV width) dispersionless modes at various energies up to 0.023 eV.²³ We shall address the issue of lattice excitations and their temperature dependence as monitored by optical experiments in more detail in a future publication.

A rather simple but very helpful description of the complete excitation spectrum may be obtained by a phenomenological approach, based on the classical dispersion theory of Drude and Lorentz.²⁴ This analysis allows to separate the various components contributing to $\sigma_1(\omega)$. We consider a number of Lorentz harmonic oscillators (HO) in order to describe the huge pseudogap-like absorption at 2.6 eV and the single low-temperature lattice mode at 0.025 eV. At frequencies below 0.4 eV, i.e., in the FIR spectral range, $\sigma_1(\omega)$ can be interpreted in terms of two components; namely a Drude-like behavior for the residual metallic conductivity for $\omega \rightarrow 0$ and a broad HO, extending from the FIR up to the visible. A much narrower HO represents the lattice mode at 0.025 eV.

The total spectral weight, i.e., $\int \sigma_1(\omega) d\omega = \frac{1}{8} \omega_p^2$, associated with the pseudogap-like absorption corresponds to a mode strength of $\omega_p \cong 8$ eV, which again is comparable to the analogous value obtained for $\text{Al}_{70}\text{Mn}_9\text{Pd}_{21}$.⁷ However, the plasma frequency with the low-frequency Drude-type component of $\sigma_1(\omega)$ characterizing the residual metallic contribution, is smaller for the present alloys than for $\text{Al}_{70}\text{Mn}_9\text{Pd}_{21}$.⁷ This is obviously consistent with the less conducting character of the Re quasicrystals (QC's). On the other hand, the parameters for the phonon modes are approximately the same for all these materials.⁷

With this phenomenological fit two energy scales may clearly be identified. First, the broad FIR to visible absorption and secondly, the resonance at 2.6 eV. This latter absorption, the onset of which occurs already at 0.4 eV and which has been ascribed to a pseudogap excitation, shifts towards higher frequencies when moving from the Mn (Ref. 7) to the Re QC's. Nevertheless, the total spectral weight encountered by these excitations remains constant for all alloys. From this trend we may infer that the electrical conductivity of quasicrystals to some extent correlates with the width of the pseudogap around the Fermi energy, particularly

when comparing the Mn and the Re compounds. However, this seems to hold only in a first approximation since, within the Re compound series a considerable change in σ_{dc} does not lead to a sizeable shift of the pseudogap absorption. This indicates that another mechanism provides a varying degree of localization in the less conducting Re materials. There is, indeed a redistribution of the total spectral weight between the effective "metallic"-like component and the nonzero frequency absorptions (i.e., FIR excitations and pseudogap excitations) in $\sigma_1(\omega)$, shown in Fig. 5.

The broad absorption centered at approximately 0.12 eV, which manifests itself via the increasing $\sigma_1(\omega)$ with increasing frequency above 0.01 eV and is part of the low-frequency tail of the pseudogap excitation, has previously been identified and was ascribed to excitations across a mobility gap.^{6,25} The authors of Ref. 6 claimed a mobility gap of about 0.025 eV, distinctly lower than the center of gravity of our low-frequency absorption. This discrepancy may be related with differences in the frequency range of available reflectivity data and the corresponding KK transformation. At any rate, the claim of a mobility gap meets with problems of consistency, at least in our case. At a mobility edge we expect a crossover from localized to delocalized states²⁵ and its presence should lead to an activated behavior of σ_{dc} in the appropriate temperature range. As is shown in Fig. 1, $\sigma_{dc}(T)$ of our samples decreases almost linearly with decreasing temperature, far from an expected exponential temperature variation. Consequently, it remains to be seen what kind of relationship may be established between the temperature dependence of σ_{dc} displayed in Fig. 1 and the dynamic part of the conductivity, which is not obvious from the present data. As an alternative scenario to the mobility-edge interpretation we suggest that a distribution of bound states is the origin for the broad low-frequency tail in $\sigma_1(\omega)$ below 0.4 eV.

IV. SUMMARY AND CONCLUSIONS

We note that the electrical transport in low-conductivity icosahedral quasicrystals reveals distinct temperature dependencies in different ranges of temperature. The linear T variation of σ at higher temperatures is compatible with a scattering rate $\tau^{-1} \sim T^{-1}$, a rather unusual feature considering the magnitude of the electrical conductivity. The $T^{1/2}$ variations of the low-temperature electrical conductivity of icosahedral $\text{Al}_{70}\text{Re}_{10}\text{Pd}_{20}$ in zero and nonzero magnetic field implies that quantum-interference effects invoking the Coulomb interaction among itinerant electrons still occur at this level of conductivity in icosahedral quasicrystals. Because of the unknown details of the electronic structure of these quasicrystals the prefactors of the $T^{1/2}$ variation of σ may not be those given in Eqs. (2) and (3). Nevertheless, the most simple analysis confirms that the density of electronic states at the Fermi energy is very low in these materials. The electrical conductivity $\sigma(T)$ of icosahedral $\text{Al}_{70}\text{Re}_{8.6}\text{Pd}_{21.4}$ saturates below 0.1 K in all applied magnetic fields up to 40 kOe, suggesting that for this material a different approach for describing the electronic transport at the lowest temperatures needs to be considered. Nevertheless, the relative reduction of $\sigma(T \rightarrow 0)$ by application of an external magnetic field is similar in magnitude in both cases. The comparison

of our $\sigma(T, H)$ results for icosahedral $\text{Al}_{70}\text{Re}_{10}\text{Pd}_{20}$ and $\text{Al}_{70}\text{Re}_{8.6}\text{Pd}_{21.4}$ indicates that the breakdown of the quantum-interference-type behavior in Al-Re-Pd quasicrystals occurs within the *metallic regime* of conductance, at a residual conductivity value in the range between 1.7 and $30 \Omega^{-1} \text{cm}^{-1}$. Although an insulating ground state in Al-Re-Pd quasicrystals in a narrow range of the phase diagram seems possible,³ our $\sigma(T, H)$ data for $\text{Al}_{70}\text{Re}_{8.6}\text{Pd}_{21.4}$ suggests that corresponding claims should be based on measurements at very low temperatures, i.e., below 0.1 K at least.

A common feature in $\sigma_1(\omega)$ of these quasicrystals of the type Al-*T*-Pd, where *T* is Mn or Re, respectively, is the large absorption in the visible spectral range, which is ascribed to excitations across a pseudogap in the electronic excitation spectrum. More puzzling is the broad absorption in the FIR and mid-IR spectral range which, because of the the $\sigma_{\text{dc}}(T)$ data, we believe cannot be ascribed to a mobility-gap feature⁶ in our case.

The energies of the optical modes of lattice excitations in these icosahedral quasicrystals seem not to be very sensitive to the replacement of manganese by rhenium. Optical lattice

modes in icosahedral $\text{Al}_{70}\text{Re}_{10}\text{Pd}_{20}$, $\text{Al}_{70}\text{Re}_{8.6}\text{Pd}_{21.4}$ as well as Al-Mn-Pd quasicrystals are observed at energies close to 0.03 eV.^{7,23} The acoustical phonons are again hardly much different, because the Debye temperature extracted from the low-temperature specific heat for $\text{Al}_{70}\text{Mn}_9\text{Pd}_{21}$ (Ref. 26) of $\Theta_D = 362$ K is very close to the values of $\Theta_D = 382$ K and $\Theta_D = 378$ K reported for $\text{Al}_{70}\text{Re}_{10}\text{Pd}_{20}$ (Ref. 17) and $\text{Al}_{70}\text{Re}_{8.6}\text{Pd}_{21.4}$,¹³ respectively. Finally we note a peculiar temperature dependence of an optical lattice excitation of the Al-Re-Pd quasicrystals which seems not to have been reported before.

ACKNOWLEDGMENTS

We acknowledge useful discussions with M. de Boissieu, K. Edagawa, C. Janot, P. Kalugin, and P. Weinberger and we would like to thank S. Ritsch and P. Wägli for the sample characterization by electron microscopy and J. Müller for technical assistance. This work was financially supported in part by the Schweizerische Nationalfonds zur Förderung der Wissenschaftlichen Forschung.

-
- ¹H. Akiyama, Y. Honda, T. Hashimoto, K. Edagawa, and S. Takeuchi, *Jpn. J. Appl. Phys.* **32**, L1003 (1993).
²Y. Honda, K. Edagawa, A. Yoshioka, T. Hashimoto, and S. Takeuchi, *Jpn. J. Appl. Phys.* **33**, 4929 (1994).
³S. J. Poon, F. S. Pierce, and Q. Guo, *Phys. Rev. B* **51**, 2777 (1995).
⁴P. Lindqvist, P. Lanco, C. Berger, A. G. M. Jansen, and F. Cyrot-Lackmann, *Phys. Rev. B* **51**, 4796 (1995).
⁵T. Grenet, P. Lindqvist, C. Berger, C. Gignoux, and A. G. M. Jansen, in *Quasicrystals. Proceedings of the 5th International Conference, Avignon, France, 22–26 May 1995*, edited by C. Janot and R. Mosseri (World Scientific, Singapore, 1995).
⁶D. N. Basov, F. S. Pierce, P. Volkov, S. J. Poon, and T. Timusk, *Phys. Rev. Lett.* **73**, 1865 (1994).
⁷L. Degiorgi, M. A. Chernikov, C. Beeli, and H. R. Ott, *Solid State Commun.* **87**, 721 (1993).
⁸B. L. Altshuler and A. G. Aronov, in *Electron-Electron Interactions in Disordered Systems*, edited by V. M. Agranovich and A. A. Maradudin (North-Holland, Amsterdam, 1985), p. 690.
⁹P. A. Lee and T. V. Ramakrishnan, *Rev. Mod. Phys.* **57**, 287 (1985).
¹⁰L. P. Gor'kov, A. I. Larkin, and D. E. Khmel'nitskii, *JETP Lett.* **30**, 228 (1979).
¹¹G. A. Thomas, A. Kawabata, Y. Ootuka, S. Katsumoto, S. Kobayashi, and W. Sasaki, *Phys. Rev. B* **26**, 2113 (1982).
¹²T. F. Rosenbaum, R. F. Milligan, M. A. Paalanen, G. A. Thomas, R. N. Bhatt, and W. Lin, *Phys. Rev. B* **27**, 7509 (1983).
¹³M. A. Chernikov, A. D. Bianchi, E. Felder, U. Gubler, and H. R. Ott, *Europhys. Lett.* **35**, 431 (1996).
¹⁴W. A. Phillips, *J. Low Temp. Phys.* **7**, 351 (1972).
¹⁵P. W. Anderson, B. I. Halperin, and C. M. Varma, *Philos. Mag.* **25**, 1 (1972).
¹⁶R. O. Pohl, in *Amorphous Solids: Low-Temperature Properties*, edited by W. A. Phillips (Springer-Verlag, Berlin, 1981), p. 167.
¹⁷E. Felder, A. D. Bianchi, M. A. Chernikov, and H. R. Ott (unpublished).
¹⁸S. E. Burkov, T. Timusk, and N. W. Ashcroft, *J. Phys. Condens. Matter* **4**, 9447 (1992).
¹⁹S. E. Burkov, A. A. Varlamov, and D. V. Livanov, *JETP Lett.* **62**, 361 (1995).
²⁰S. E. Burkov, A. A. Varlamov, and D. V. Livanov, *Phys. Rev. B* **53**, 11 504 (1996).
²¹A. N. Ionov and I. S. Shlimak, *JETP Lett.* **35**, 196 (1982).
²²J.-B. Suck, *J. Non-Cryst. Solids* **153&154**, 573 (1993).
²³M. Boudard, M. de Boissieu, S. Kycia, A. I. Goldman, B. Hennion, R. Bellissent, M. Quilichini, R. Currat, and C. Janot, *J. Phys. Condens. Matter* **7**, 7299 (1995).
²⁴F. Wooten, *Optical Properties of Solids* (Academic, New York, 1972).
²⁵N. F. Mott and E. A. Davis, *Electronic Processes in Non-crystalline Materials* (Clarendon, Oxford, 1971).
²⁶M. A. Chernikov, A. Bernasconi, C. Beeli, A. Schilling, and H. R. Ott, *Phys. Rev. B* **48**, 3058 (1993).